node (Fig. 3I). Additionally, after the surgical treatment, a brain metastasis of the adenocarcinoma was observed in the patient. The above findings suggest that CD74-ROS1 fusion transcripts are expressed in a subset of NSCLCs.

We next examined whether the NSCLC case containing the CD74-ROS1 fusion transcripts also contained previously reported driver mutations. Mutation cluster regions for *KRAS*, *EGFR*, *BRAF* and *PIK3CA* (18-20) were searched for somatic mutations and the expression of EML4-ALK and KIF5B-ALK fusion transcripts (1-5) was examined; however, no somatic mutations in exons 2 and 3 of *KRAS*, exons 19 and 21 of *EGFR*, exons 11 and 15 of *BRAF*, or exons 9 and 20 of *PIK3CA* and no expression of EML4-ALK or KIF5B-ALK fusion transcripts were detected. We also performed a mutational analysis of the entire coding region of *p53* of the carcinoma that contained CD74-ROS1 fusion transcripts. The case was found to be heterozygous for the Arg and Pro alleles of the *p53* p.Arg72Pro genetic polymorphism, which is associated with a functional difference (21); however, no somatic *p53* mutations were detected.

## Discussion

In the present study, the expression of CD74-ROS1 fusion transcripts was found in one (0.9%) of the 114 NSCLCs that were examined, but the expression of SLC34A2-ROS1, EZR-ROS1, or KIF5B-RET fusion transcripts was not detected in any of the NSCLCs. The detected fusion occurred between exon 6 of CD74 and exon 34 of ROS1 and was observed in a non-smoker female. Histologically, the carcinoma was an adenocarcinoma with a predominant acinar pattern; a mucinous cribriform pattern and a solid signet-ring cell pattern were also observed in a portion of the adenocarcinoma. ROS1 protein was overexpressed in a cancer-specific manner at both the primary site and the lymph node metastases. No somatic mutations were detected in the mutation cluster regions of the *KRAS*, *EGFR*, *BRAF* and *PIK3CA* genes and the entire coding region of *p53* in the carcinoma, and the expression of EML4- and KIF5B-ALK fusions was also not detected. These results suggest that CD74-ROS1 fusion contributes to the carcinogenesis of this NSCLC case as a driver mutation.

To date, ROS1 fusion transcripts have been detected in 0.7-1.9% of NSCLC patients (Chinese, Japanese, white and Caucasian populations) (5,9,10,12,14,15,17). The analytical methods used in the above-mentioned reports varied and RT-PCR, fluorescence *in situ* hybridization and immunohistochemical analyses have been used to search for NSCLCs containing ROS1 fusion products (5,9,10,12,14,15,17). Considering our results (0.9% of Japanese NSCLC patients) and the results of the above-mentioned previous papers, racial differences in the frequency of ROS1 fusion-positive NSCLC are thought to be minimal, although distinct analytical methods were used in the various reports. Approximately 1.6 million new lung cancers are diagnosed each year worldwide (22); if NSCLC comprises 90% of these cancers, 1.45 million new cases of NSCLC are diagnosed every year. Since the prevalence of ROS1 fusion is ~1% of all NSCLCs, ~14,500 new patients have ROS1 fusion-positive NSCLC. Recently, ROS1 inhibition was shown to lead to the suppression of the proliferation of cells containing ROS1 fusion *in vitro* (12,14); furthermore, crizotinib, a small molecule inhibitor against ROS1 kinase in addition to ALK kinase, was shown to exhibit antitumor properties in a patient with NSCLC containing an ROS1 fusion (12,14). Thus, patients with ROS1 fusion-positive NSCLC may comprise a novel subclass that could benefit clinically from ROS1 inhibition.

In our CD74-ROS1 fusion-positive case, no other oncogenic driver mutations were detected. Oncogenic driver mutations are responsible for the initiation and progression of NSCLCs, and they differ from passenger mutations in that they are also found within the cancer genomes but exist as a by-product of cancer cell development (10,13,18,19). In general, oncogenic driver mutations are mutually exclusive (10). ROS1 fusion-positive cases reported in two previous studies (4,17) were negative for alterations in the *ALK*, *RET*, *EGFR* and *KRAS* genes. Thus, our results for the driver mutation search are compatible with the results of these previous reports, suggesting that ROS1 fusion is mutually exclusive with other oncogenic driver mutations in NSCLC.

A mucinous cribriform pattern and a solid signet-ring cell pattern were observed in a portion of the adenocarcinoma in the present case. Yoshida *et al* (17) recently reported that one-third of ROS1 fusion-positive NSCLCs contain a mucinous cribriform pattern and one-third contain a solid signet-ring cell pattern. Of note, both patterns are frequently observed in ALK-rearranged NSCLC (4,23,24). Thus, both a mucinous cribriform pattern and a solid signet-ring cell pattern may be common pathohistological characteristics of ROS1 and ALK fusion-positive NSCLCs. We also showed that the ROS1 protein was highly expressed in both histological patterns in our case, and an increased ROS1 protein expression in both components has not previously been demonstrated, suggesting a novel finding of the present study. These results indicate that ROS1 is involved in the morphogenesis of the patterns.

*EGFR* mutations and EML4-ALK fusions are preferentially associated with NSCLC in non-smokers (4,18,19). Our CD74-ROS1 fusion-positive case was a never-smoker. In three previous reports, ROS1 fusion was frequently found in the NSCLCs of never-smokers (4,12,17); however, this characteristic was not detected in another report (14). The accumulation of ROS1 fusion-positive cases with information on the smoking history is required to better understand the role of ROS1 fusion in NSCLCs.

In conclusion, our CD74-ROS1 fusion-positive NSCLC in conjunction with previously detected ROS1 fusion-positive NSCLCs suggested that ROS1 fusion is involved in the carcinogenesis of a subset of NSCLCs and may significantly aid in elucidating the characteristics of ROS1 fusion-positive NSCLC in the future.

## Acknowledgements

The authors acknowledge Ms. S. Izumo (Hamamatsu University School of Medicine) for her technical assistance. The present study was supported in part by a Grant-in-Aid from the Ministry of Health, Labour and Welfare (21-1), a Grant-in-Aid from the Japan Society for the Promotion of Science (22590356), a Grant-in-Aid from the Ministry of Education, Culture, Sports, Science and Technology (221S0001) and the Smoking Research Foundation.

## References


1. Soda M, Choi YL, Enomoto M, Takada S, Yamashita Y, Ishikawa S, Fujiwara S, Watanabe H, Kurashina K, Hatanaka H, Bando M, Ohno S, Ishikawa Y, Aburatani H, Niki T, Sohara Y, Sugiyama Y and Mano H: Identification of the transforming EML4-ALK fusion gene in non-small-cell lung cancer. Nature 448: 561-566, 2007.
2. Shinmura K, Kageyama S, Tao H, Bunai T, Suzuki M, Kamo T, Takamochi K, Suzuki K, Tanahashi M, Niwa H, Ogawa H and Sugimura H: EML4-ALK fusion transcripts, but no NPM-, TPM3-, CLTC-, ATIC-, or TFG-ALK fusion transcripts, in non-small cell lung carcinomas. Lung Cancer 61: 163-169, 2008.
3. Shinmura K, Kageyama S, Igarashi H, Kamo T, Mochizuki T, Suzuki K, Tanahashi M, Niwa H, Ogawa H and Sugimura H: EML4-ALK fusion transcripts in immunohistochemically ALK-positive non-small cell lung carcinomas. Exp Ther Med 1: 271-275, 2010.
4. Takeuchi K, Soda M, Togashi Y, Suzuki R, Sakata S, Hatano S, Asaka R, Hamanaka W, Ninomiya H, Uehara H, Lim Choi Y, Satoh Y, Okumura S, Nakagawa K, Mano H and Ishikawa Y: RET, ROS1 and ALK fusions in lung cancer. Nat Med 18: 378-381, 2012.
5. Lipson D, Capelletti M, Yelensky R, Otto G, Parker A, Jarosz M, Curran JA, Balasubramanian S, Bloom T, Brennan KW, Donahue A, Downing SR, Frampton GM, Garcia L, Juhn F, Mitchell KC, White E, White J, Zwirko Z, Peretz T, Nechushtan H, Soussan-Gutman L, Kim J, Sasaki H, Kim HR, Park SI, Ercan D, Sheehan CE, Ross JS, Cronin MT, Jänne PA and Stephens PJ: Identification of new ALK and RET gene fusions from colorectal and lung cancer biopsies. Nat Med 18: 382-384, 2012.
6. Casaluce F, Sgambato A, Maione P, Rossi A, Ferrara C, Napolitano A, Palazzolo G, Ciardiello F and Gridelli C: ALK inhibitors: a new targeted therapy in the treatment of advanced NSCLC. Target Oncol 8: 55-67, 2013.
7. Shaw AT and Solomon B: Targeting anaplastic lymphoma kinase in lung cancer. Clin Cancer Res 17: 2081-2086, 2011.
8. O'Bryant CL, Wenger SD, Kim M and Thompson LA: Crizotinib: a new treatment option for ALK-positive non-small cell lung cancer. Ann Pharmacother 47: 189-197, 2013.
9. Rikova K, Guo A, Zeng Q, Possemato A, Yu J, Haack H, Nardone J, Lee K, Reeves C, Li Y, Hu Y, Tan Z, Stokes M, Sullivan L, Mitchell J, Wetzel R, Macneill J, Ren JM, Yuan J, Bakalarski CE, Villen J, Kornhauser JM, Smith B, Li D, Zhou X, Gygi SP, Gu TL, Polakiewicz RD, Rush J and Comb MJ: Global survey of phosphotyrosine signaling identifies oncogenic kinases in lung cancer. Cell 131: 1190-1203, 2007.
10. Li C, Fang R, Sun Y, Han X, Li F, Gao B, Iafrate AJ, Liu XY, Pao W, Chen H and Ji H: Spectrum of oncogenic driver mutations in lung adenocarcinomas from East Asian never smokers. PLoS One 6: e28204, 2011.
11. Kohno T, Ichikawa H, Totoki Y, Yasuda K, Hiramoto M, Nammo T, Sakamoto H, Tsuta K, Furuta K, Shimada Y, Iwakawa R, Ogiwara H, Oike T, Enari M, Schetter AJ, Okayama H, Haugen A, Skaug V, Chiku S, Yamanaka I, Arai Y, Watanabe S, Sekine I, Ogawa S, Harris CC, Tsuda H, Yoshida T, Yokota J and Shibata T: KIF5B-RET fusions in lung adenocarcinoma. Nat Med 18: 375-377, 2012.
12. Bergethon K, Shaw AT, Ou SH, Katayama R, Lovly CM, McDonald NT, Massion PP, Siwak-Tapp C, Gonzalez A, Fang R, Mark EJ, Batten JM, Chen H, Wilner KD, Kwak EL, Clark JW, Carbone DP, Ji H, Engelman JA, Mino-Kenudson M, Pao W and Iafrate AJ: ROS1 rearrangements define a unique molecular class of lung cancers. J Clin Oncol 30: 863-870, 2012.
13. Seo JS, Ju YS, Lee WC, Shin JY, Lee JK, Bleazard T, Lee J, Jung YJ, Kim JO, Shin JY, Yu SB, Kim J, Lee ER, Kang CH, Park IK, Rhee H, Lee SH, Kim JI, Kang JH and Kim YT: The transcriptional landscape and mutational profile of lung adenocarcinoma. Genome Res 22: 2109-2119, 2012.
14. Davies KD, Le AT, Theodoro MF, Skokan MC, Aisner DL, Berge EM, Terracciano LM, Cappuzzo F, Incarbone M, Roncalli M, Alloisio M, Santoro A, Camidge DR, Varella-Garcia M and Doebele RC: Identifying and targeting ROS1 gene fusions in non-small cell lung cancer. Clin Cancer Res 18: 4570-4579, 2012.
15. Rimkunas VM, Crosby KE, Li D, Hu Y, Kelly ME, Gu TL, Mack JS, Silver MR, Zhou X and Haack H: Analysis of receptor tyrosine kinase ROS1-positive tumors in non-small cell lung cancer: identification of a FIG-ROS1 fusion. Clin Cancer Res 18: 4449-4457, 2012.
16. Yokota K, Sasaki H, Okuda K, Shimizu S, Shitara M, Hikosaka Y, Moriyama S, Yano M and Fujii Y: *KIF5B/RET* fusion gene in surgically-treated adenocarcinoma of the lung. Oncol Rep 28: 1187-1192, 2012.
17. Yoshida A, Kohno T, Tsuta K, Wakai S, Arai Y, Shimada Y, Asamura H, Furuta K, Shibata T and Tsuda H: ROS1-rearranged lung cancer: a clinicopathologic and molecular study of 15 surgical sases. Am J Surg Pathol 37: 554-562, 2013.
18. Schmid K, Oehl N, Wrba F, Pirker R, Pirker C and Filipits M: EGFR/KRAS/BRAF mutations in primary lung adenocarcinomas and corresponding locoregional lymph node metastases. Clin Cancer Res 15: 4554-4560, 2009.
19. Pao W and Girard N: New driver mutations in non-small-cell lung cancer. Lancet Oncol 12: 175-180, 2011.
20. Ulivi P, Romagnoli M, Chiadini E, Casoni GL, Capelli L, Gurioli C, Zoli W, Saragoni L, Dubini A, Tesei A, Amadori D and Poletti V: Assessment of *EGFR* and *K-ras* mutations in fixed and fresh specimens from transesophageal ultrasound-guided fine needle aspiration in non-small cell lung cancer patients. Int J Oncol 41: 147-152, 2012.
21. Thomas M, Kalita A, Labrecque S, Pim D, Banks L and Matlashewski G: Two polymorphic variants of wild-type p53 differ biochemically and biologically. Mol Cell Biol 19: 1092-1100, 1999.
22. Jemal A, Bray F, Center MM, Ferlay J, Ward E and Forman D: Global cancer statistics. CA Cancer J Clin 61: 69-90, 2011.
23. Rodig SJ, Mino-Kenudson M, Dacic S, Yeap BY, Shaw A, Barletta JA, Stubbs H, Law K, Lindeman N, Mark E, Janne PA, Lynch T, Johnson BE, Iafrate AJ and Chirieac LR: Unique clinicopathologic features characterize ALK-rearranged lung adenocarcinoma in the western population. Clin Cancer Res 15: 5216-5223, 2009.
24. Jokoji R, Yamasaki T, Minami S, Komuta K, Sakamaki Y, Takeuchi K and Tsujimoto M: Combination of morphological feature analysis and immunohistochemistry is useful for screening of EML4-ALK-positive lung adenocarcinoma. J Clin Pathol 63: 1066-1070, 2010.

SCIENTIFIC REPORTS

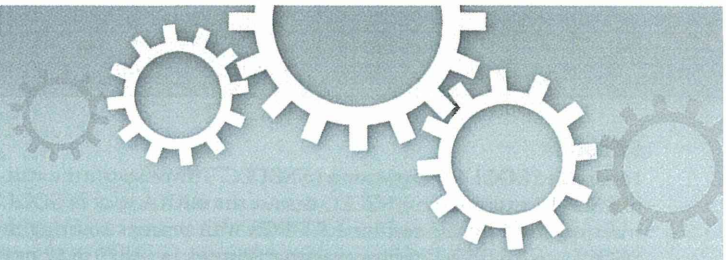

OPEN

SUBJECT AREAS:
NON-SMALL-CELL LUNG CANCER
BIOMARKER RESEARCH

Received
1 May 2013

Accepted
2 October 2013

Published
22 October 2013

Correspondence and requests for materials should be addressed to H.S. (hsugimur@hama-med.ac.jp)

# SGOL1 variant B induces abnormal mitosis and resistance to taxane in non-small cell lung cancers

Shun Matsuura[1,2], Tomoaki Kahyo[1], Kazuya Shinmura[1], Moriya Iwaizumi[1], Hidetaka Yamada[1], Kazuhito Funai[3], Jun Kobayashi[4], Masayuki Tanahashi[5], Hiroshi Niwa[5], Hiroshi Ogawa[6], Takashi Takahashi[7], Naoki Inui[2], Takafumi Suda[2], Kingo Chida[2], Yoshinori Watanabe[8] & Haruhiko Sugimura[1]

[1]Department of Tumor Pathology, Hamamatsu University School of Medicine, 1-20-1 Handayama, Higashi-ku, Hamamatsu, Shizuoka, 431-3192, Japan, [2]Second Division, Department of Internal Medicine, Hamamatsu University School of Medicine, 1-20-1 Handayama, Higashi-ku, Hamamatsu, Shizuoka, 431-3192, Japan, [3]First Department of Surgery, Hamamatsu University School of Medicine, 1-20-1 Handayama, Higashi-ku, Hamamatsu, Shizuoka, 431-3192, Japan, [4]Thoracic Surgery, Shimada Municipal Hospital, 1200-5 Noda, Shimada, Shizuoka, 427-8502, Japan, [5]Division of Thoracic Surgery, Respiratory Disease Center, [6]Division of Pathology, Seirei Mikatahara General Hospital, 3453 Mikatahara, Kita Ward, Hamamatsu, Shizuoka, 433-8558, Japan, [7]Department of Molecular Carcinogenesis, Nagoya University Graduate School of Medicine, 65 Tsurumai-cho, Showa-ku, Nagoya, Aichi, 466-8550, Japan, [8]Laboratory of Chromosome Dynamics, Institute of Molecular and Cellular Biosciences, University of Tokyo, Yayoi, Tokyo, 113-0032, Japan.

**Mitosis is the most conspicuous cell cycle phase and Shugoshin-like 1 (SGOL1) is a key protein in protecting sister chromatids from precocious separation during mitosis. We studied the role of SGOL1 and its splice variants in non-small cell lung cancer (NSCLC) using 82 frozen NSCLC tissue samples. SGOL1-B expression was prevalent in smokers, in cases with a wild-type (WT) EGFR status, and in cases with the focal copy number amplification of genes that are known to be important for defining the biological behaviors of NSCLC. The overexpression of SGOL1-B1 in an NSCLC cell line induced aberrant chromosome missegregation, precociously separated chromatids, and delayed mitotic progression. A higher level of SGOL1-B mRNA was related to taxane resistance, while the forced downregulation of SGOL1-B increased the sensitivity to taxane. These results suggest that the expression of SGOL1-B causes abnormal mitosis and taxane resistance in NSCLC cells.**

Shugoshin-like protein (SGOL1), one of the human homologs of yeast shugoshin, is localized in the centromeric region and prevents the precocious cleavage of the cohesion complex at the centromere[1]. SGOL1 is crucial for mitotic progression and chromosome segregation. In a study on human cancer, we found that SGOL1 expression was decreased in colorectal cancer and that SGOL1-knockdown led to chromosome instability (CIN) in a colon cancer cell line[2]. In general, many tumor-specific splicing variants have been studied in a variety of tumors. SGOL1 variants have been previously identified, and these variants appear to have a negative effect on the cohesion between sister chromatids[3], with SGOL1-P1 causing abnormal mitosis and unstable chromatid cohesion in colon cancer[4]. However, the role of SGOL1 splice variants in human cancer is generally unknown.

Lung cancer is a leading cause of cancer mortality in many countries[5]. Detailed molecular and biological characterization of certain types of NSCLC has provided better guidance in clinical management[6–8], that is, targeted therapies and individualized treatments. Taxanes (*e.g.*, docetaxel and paclitaxel), disrupters of microtubule, are commonly used for the treatment of advanced NSCLC[9]. The efficacy of taxanes against cancer cells can be attributed to mitotic arrest resulting in mitotic catastrophe, promoting cell death during metaphase or death preceded by multinucleation[10]. However, the strategies that resistant tumor cells use to evade death induced by taxanes are also unclear. The cell machinery involved in mitosis control may be involved in taxane resistance of cancer cells.

In this study, we evaluated the expression levels of SGOL1 mRNA in clinical NSCLC specimens and investigated the malfunction of SGOL1-B, a tumor-specific variant, in NSCLC cells. Furthermore, we investigated whether the SGOL1-B expression level defines the response of NSCLC cells to taxanes.

## Results

**Increased SGOL1-B expression in NSCLC.** To investigate the status of SGOL1 expression in NSCLC tissues, the mRNA level of SGOL1 was quantified using real-time RT-PCR with primers covering the SGOL1-A, -B, and -C splicing variants (Figures 1a and b) in 82 pairs of primary NSCLC and matched normal tissues located adjacent to the carcinoma. Increased SGOL1 expression (T > N) was observed in 62 (75.6%) of the 82 NSCLCs (Figure 1c); moreover, a significant difference was detected in the mRNA expression level of SGOL1 between cancerous and non-cancerous tissue using a statistical analysis ($P < 0.0001$ according to a Wilcoxon matched pairs test). This result suggests that SGOL1 expression is upregulated in NSCLC.

Since several splicing variants of SGOL1 exist (Figure 1a), we next examined whether the mRNA expression of each SGOL1 variant was upregulated in the 82 NSCLCs. We compared the expression level of each SGOL1 variant in matched pairs of cancerous and non-cancerous tissues. A paired comparison in all cases revealed a statistically significant increase in the expression of SGOL1-B, but not of SGOLI-A or SGOLI-C, in the cancerous tissue, compared with the non-cancerous tissues (Figure 1d, $P = 0.047$). Very interestingly, all the cancers expressing SGOL1-B ($n = 24$) showed increased expression levels in the cancerous tissue, compared with the non-cancerous tissue (cancer tissue-specific expression). We analyzed the contributions of other SGOL1 isoforms to the phenotype exerted by SGOL1-B1 expression. In SGOL1-B expressing cases, the ratio SGOL1-A/SGOL-B is larger than 1.0 while SGOL1-C/SGOL1-B is lower than 1.0 (Supplementary Table S1 online). These results suggest that SGOL1-B has an important role in the carcinogenesis of NSCLC; therefore, we focused on SGOL1-B in the subsequent studies.

**Association of SGOL1-B expression with EGFR status and focal copy number amplifications in NSCLC.** Next, we investigated whether the levels of SGOL1-B mRNA expression were associated with the clinicopathological features in NSCLC patients (Table 1). The frequencies of patients with smoking history and WT EGFR were statistically higher in the group with SGOL1-B-positive cancer than in the group with SGOL1-B-negative cancer ($P = 0.029$ and $P = 0.017$, respectively). No associations were found between the clinicopathological factors of sex, onset age, tumor pathology, or tumor stage and the status of SGOL1-B mRNA expression in the cancerous tissue.

Then, we hypothesized that SGOL1-B-positive lung cancers may have more frequent and extensive genomic alterations. To assess the association between SGOL1-B expression and genetic alterations, we selected five DNA targets commonly amplified in lung cancer, i.e., 8p12 (FGFR1), 3q26.3-q27 (SOX2 and PIK3CA), 7q31.1 (MET), and 7p12 (EGFR), and evaluated their gene copy changes using FISH in a tissue microarray[11–15]. A specific relationship was not observed between SGOL1-B expression and focal copy number amplification at a particular locus, but focal copy number amplifications at one of these loci were identified in 18 of the 58 (31.0%) patients with SGOL1-B negative cancer and in 13 of the 24 (54.2%) patients with SGOL1-B positive cancer ($P = 0.049$, Table 1). The mechanisms of these focal copy number amplifications are not known, but SGOL1-B-positive cancer represents a subset of lung cancers with focal copy number amplifications.

**SGOL1-B1 is localized at centromeres, and SGOL1-B1 overexpression exhibits aberrant chromosome-alignment during mitosis in lung cancer cells.** To characterize the effect of SGOL1-B expression in NSCLC, the lung adenocarcinoma cell line ACC-LC-176 was transfected with an expression vector for MYC-tagged SGOL1-B1. The overexpression of MYC-SGOL1-B1 was confirmed in ACC-LC-176 cells using a western blot analysis (Figure 2a). An immunofluorescence analysis revealed that SGOL1-B1 was localized in the nucleus during interphase and mitosis (Figure 2b). To further investigate the specific localization of SGOL1-B1, we performed a co-immunofluorescence study for the centromere and MYC-SGOL1-B1. MYC-SGOL1-B1 was clearly localized at the centromere in SGOL1-B1-overexpressing cells (Figure 2c). Furthermore, when we focused on the chromosome positioning morphology during mitosis, chromosome missegregation in pro-metaphase was more frequently observed in SGOL1-B1-overexpressing cells than in empty-vector transfected cells (66.7% vs. 6.8%) (Figure 2c). These results suggested that SGOL1-B1 overexpression is associated with mitotic abnormalities. Furthermore, we tested to see if the overexpression of SGOL1-A1 rescued the phenotype induced by the overexpression of SGOL1-B1. The chromosome missegregation induced by SGOL1-B1 was partially dismissed in the presence of SGOL1-A1 (Figure 2d). Since multiple spindle poles have been reported to be common in mitotic SGOL1-knockdown cells (1), we examined the cells for the presence of centrosome amplification (an extra centrosome; more than 3 centrosomes). Centrosome amplification was observed more frequently in the ACC-LC-176 cells expressing SGOL1-B1 than in the vector control cells (Figure 2e). All these results suggested that SGOL1-B1 is localized at the centromere and that the overexpression of SGOL1-B1 exhibits aberrant chromosome-alignment in lung cancer cells.

**Cohesion defect and mitotic progression delay in lung cancer cells expressing SGOL1-B1.** SGOL1 is recognized as a centromeric protector in somatic cells during mitosis (1). To assess the effect of SGOL1-B1 on sister chromatid cohesion in lung cancer cells, a chromosome spread assay was performed in the ACC-LC-176 cell line. Spread chromosomes were stained with DAPI, and the frequency of each of the separation patterns was counted (Figure 3a). As a positive control for this experiment, SGOL1 knockdown was also performed using shRNA plasmids targeting SGOL1-A, SGOLI-B, and SGOL1-C, as reported previously (3). Severe cohesion defects were observed significantly more frequently in SGOL1-B1-expressing cells (22%) and SGOL1-knockdown cells (31%) than in control cells (7%) (Figure 3b). These results suggest that SGOL1-B induces the precocious separation of sister chromatids in lung cancer cells. We next monitored the mitotic progression in SGOL1-B1-expressing ACC-LC-176 cells, SGOL1-knockdown cells, and control cells using time-lapse microscopy. The chromosomal masses separated without congressing at the metaphase plate in some percentage of the SGOL1-B1-transfected cells and SGOL1-knockdown cells; however, no such cells were observed in empty vector-transfected cells (Figure 3c and Supplementary Movie 1-3 online). We measured the time from nuclear envelop breakdown (NEBD) to the anaphase transition. The median time was 33.1 minutes in the SGOL1-B1-transfected cells (range, 28.6 to 37.5 minutes) compared with 25.1 minutes in the empty vector-transfected control cells (range, 20.5 to 29.6 minutes) (Figure 3d). The prolongation of the time from NEBD until anaphase onset was also observed in SGOL1-knockdown cells (range, 39.9 to 48.8 minutes; median, 44.4 minutes) (Figure 3d). These results indicate that SGOL1-B1 overexpression, as well as SGOL1-knockdown, prevent chromosomes from a proper alignment to the metaphase plate in lung cancer cells, resulting in a delay of anaphase onset.

**Association between SGOL1-B expression and the response to taxanes in NSCLC cells with WT EGFR.** Despite the recent development of various new drugs targeting specific molecules, anti-mitotic drug taxanes are still the mainstay of treatment for advanced NSCLC with WT EGFR. Since an association between the WT EGFR status and SGOL1-B expression was observed in Table 1, we examined whether the expression status of SGOL1-B was associated with the sensitivity to taxanes, such as docetaxel or paclitaxel. First, the mRNA expression levels of SGOL1-B were determined in three NSCLC cell lines with WT EGFR and a NSCLC cell line with EGFR mutation. The SGOL1-B expression levels were low in PC-3 and A549 cells

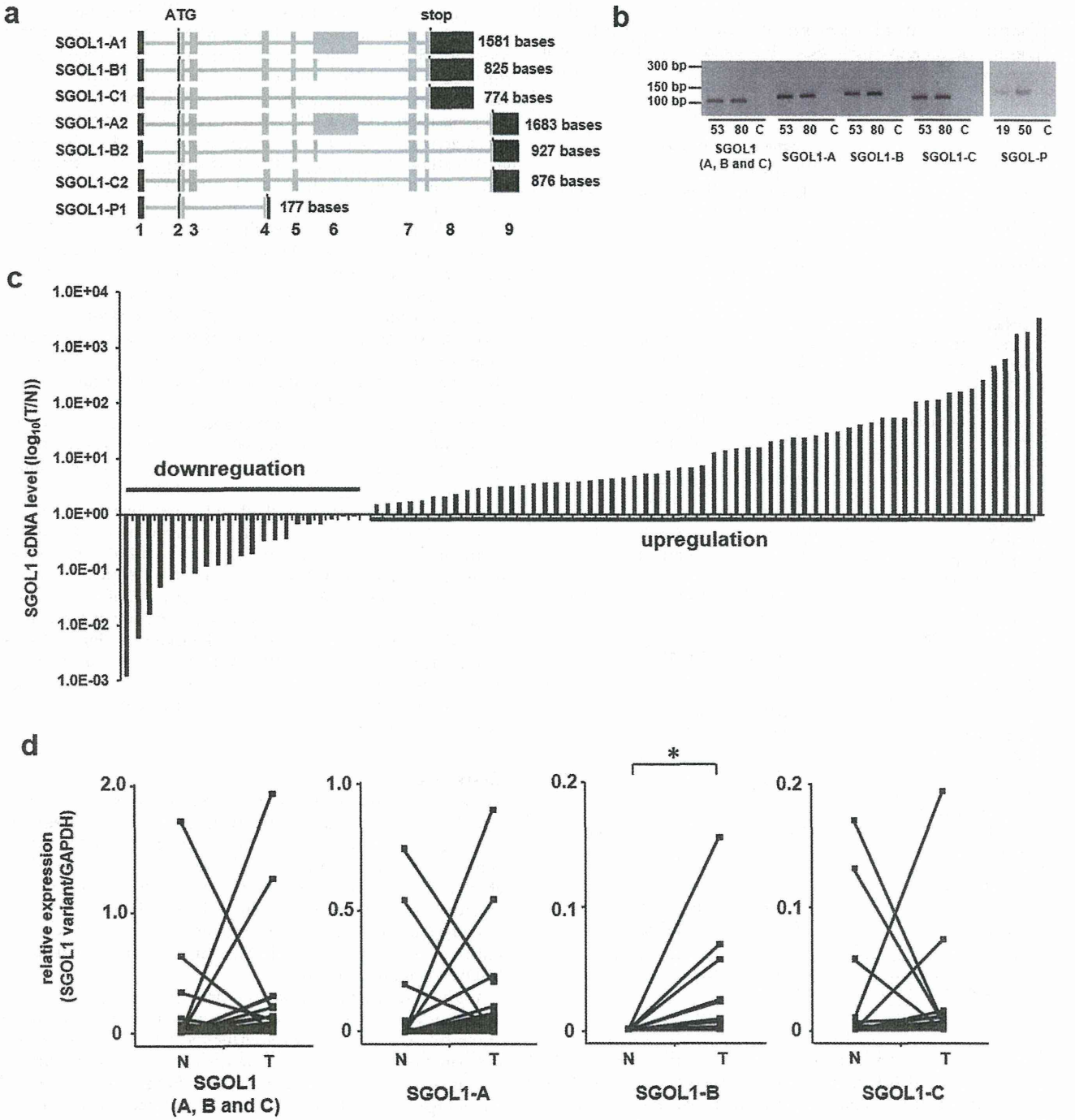


**Figure 1 | Expression of SGOL1 variants in NSCLC tissue.** (a) Scheme of SGOL1 transcript variants. The filled boxes represent exons (exons 1–9). The coding region is indicated in gray, and the non-coding region is indicated in black. The number at the right indicates the length of the protein coding sequence. (b) Amplified products of various SGOL1 transcripts using quantitative real-time RT-PCR. Specific primers for each SGOL1 variant (A, B, C, and P) or primers targeting variants A, B, and C were used for the PCR. After the quantitative real-time RT-PCR reaction using a LightCycler instrument, the PCR products were electrophoresed and stained with ethidium bromide in an agarose gel to confirm the production of objective products. The number and "C" below the panel indicate the case number and negative control, respectively. (c) Measurement of the SGOL1 mRNA expression levels in 82 paired human NSCLC and normal lung tissues using quantitative real-time RT-PCR. Expression of SGOL1 transcripts containing variants A, B, and C. After normalizing the expression levels of SGOL1 to those of GAPDH, the T/N values were calculated by dividing the amount of normalized transcripts in the tumor tissue by the amount in the corresponding normal lung tissue. Cases were grouped into two categories according to their T/N value: SGOL1 downregulation ($T/N < 1$) and SGOL1 upregulation ($T/N > 1$). Differences between the normalized SGOL1 mRNA level in the tumor tissue and the corresponding normal tissue were statistically analyzed using the Wilcoxon matched pairs test, and the *P*-value was less than 0.0001. Data were calculated from triplicate measurements. (d) Paired comparison of mRNA expression from normal and tumor samples in each SGOL1 splice variant in all cases. $^*P < 0.05$ (Student *t*-test).

Table 1 | Clinicopathological and molecular features of 82 NSCLC patients according to the SGOL1-B expression status in their carcinoma

| | SGOL1-B expression status | | |
|---|---|---|---|
| | Positive $n = 24$ | Negative $n = 58$ | |
| Factors | Number (%) | Number (%) | *P*-value |
| Gender | | | |
| Male | 18 (75.0%) | 37 (63.8) | 0.326 |
| Female | 6 (25.0%) | 21 (36.2) | |
| Age | | | |
| Median | 67 | 67 | |
| Smoking | | | |
| Current/ex-smoker | 22 (91.7) | 40 (69.0) | 0.029 |
| Never smoker | 2 (8.3) | 18 (31.0) | |
| Pathology | | | |
| Adenocarcinoma | 9 (37.5) | 37 (63.8) | 0.057 |
| Squamous cell carcinoma | 12 (50.0) | 19 (32.8) | |
| Others | 3 (12.5) | 2 (3.4) | |
| Stage | | | |
| 1–2 | 14 (58.3) | 44 (75.8) | 0.119 |
| 3–4 | 10 (41.7) | 14 (24.2) | |
| EGFR status | | | |
| Wild-type | 23 (95.8) | 42 (72.4) | 0.017 |
| Mutation type* | 1 (4.2) | 16 (27.6) | |
| FGFR1 copy number | | | |
| normal | 23 (95.8) | 54 (93.1) | 0.634 |
| amplification | 1 (4.2) | 4 (6.9) | |
| SOX2 copy number | | | |
| normal | 19 (79.2) | 52 (89.7) | 0.205 |
| amplification | 5 (20.8) | 6 (10.3) | |
| PIK3CA copy number | | | |
| normal | 17 (70.8) | 48 (82.8) | 0.226 |
| amplification | 7 (29.2) | 10 (17.2) | |
| MET copy number | | | |
| normal | 21 (87.5) | 55 (94.8) | 0.246 |
| amplification | 3 (12.5) | 3 (5.2) | |
| EGFR copy number | | | |
| normal | 20 (83.3) | 53 (91.4) | 0.289 |
| amplification | 4 (16.7) | 5 (8.6) | |
| Focal copy number *amplifications*** | | | |
| negative | 11 (45.8) | 40 (69.0) | 0.049 |
| positive | 13 (54.2) | 18 (31.0) | |

*EGFR mutation type: either the exon 19 deletion or L858R point mutation in exon 21.
**focal copy number amplifications were identified in at least one of the five genomic alterations (FGFR1, SOX2, PIK3CA, MET, or EGFR amplification).

compared with H1299 and ACC-LC-176 cells (Figure 4a). We next performed a growth inhibition assay to test the sensitivity of these cells to taxanes. The treatment with clinically relevant concentrations of docetaxel or paclitaxel resulted in the robust inhibition of cell viability in PC-3 and A549 cells, compared with that in H1299 and ACC-LC-176 cells (Figure 4b). This result suggests that the increased expression of SGOL1-B is associated with increased taxane resistance. Taxanes are known to promote cell death by inducing a potent mitotic block, resulting from the accumulation of cells at the G2-M phase of the cell cycle[16]. To further examine the morphological phenotype of cells with different SGOL1-B expression levels when exposed to 1,000 nM of docetaxel, we performed time-lapse microscopy using 4 cell lines expressing H2B-GFP fusion protein as a nuclear marker. We used the terms "death in interphase" for the processes in which the cells died in interphase before entering mitosis and "death in mitosis" for the processes in which the cells activate a death pathway while still in mitosis, according to the terminology used in a previous paper (Figure 4c and Supplementary Movie 4–5 online)[17]. 83.1% of the A549 cells and 72.3% of the PC-3 cells exhibited "death in interphase", whereas the H1299 cells exhibited more variable fates, with 26.8% of the cells exhibiting "death in interphase" and 64.9% of the cells exhibiting "death in mitosis" after prophase-metaphase arrest (Figure 4d). Moreover, a substantial proportion of the ACC-LC-176 cells exhibited "death in mitosis", indicating that they was unable to progress to cell division and died during mitosis (Figure 4d). These results suggest that the process of mitotic catastrophe caused by taxane treatment is associated with the expression level of SGOL1-B.

To exclude the possibility that differences other than the SGOL1-B expression level between A549 and ACC-LC-176 cells affect the taxane response, we examined the effect of SGOL1-B1 overexpression on taxane resistance in A549 cells. The ectopic overexpression of SGOL1-B1 enhanced the cellular viability after treatment with docetaxel or paclitaxel in A549 cells (Figure 5a). We next performed time-lapse microscopy to examine A549 cells expressing SGOL1-B1 and measured the rate of each type of cell death caused by treatment with 1,000 nM of docetaxel. Strikingly, the proportion of cells exhibiting "death in mitosis" was markedly increased by SGOL1-B1 overexpression (2.6% in control cells vs. 25.0% in cells overexpressing SGOL1-B1) (Figure 5b and Supplementary Movie 6 online). Next, we performed the knockdown of SGOL1-B in ACC-LC-176 cells to examine the role of abundant endogenous SGOL1-B. Western blotting confirmed the downregulation of SGOL1-B expression (Figure 5c). The decrease in the SGOL1-B expression level led to an increased sensitivity of ACC-LC-176 cells to docetaxel and paclitaxel (Figure 5d). Moreover, the proportion of cells exhibiting "death in interphase" after treatment with 1,000 nM of docetaxel was markedly increased by SGOL1-B1 knockdown (Figure 5e and Supplementary Movie 7 online). A similar result was obtained in H1299 cells (Supplementary Figure S1 online). These results suggest that the SGOL1-B expression level defines taxane resistance in NSCLC with WT EGFR.

## Discussion

The key findings of our study are that SGOL1 expression is upregulated in NSCLC and that the upregulation of SGOL1-B is associated with ominous clinical feature such as having WT EGFR and focal copy number amplification. SGOL1-B1 overexpression induced aberrant chromosome alignment during mitosis, the precocious separation of sister chromatids, and a delay in the onset of anaphase in lung cancer cells. Furthermore, taxane-resistance in lung cancer cells was shown to be associated with an elevated expression of SGOL1-B and mitotic arrest.

We have shown that SGOL1 was predominantly expressed in the tumorous regions of lung tissues, relative to normal tissues contrasting to the case of colon cancer, in which SGOL1 is downregulated, compared with its expression in normal tissues[2]. It is not surprising because gene expression patterns often differ among cancers in different organs[18-21], but we do not know the implication of this difference in SGOL1 expression profile at this moment.

Genomic amplifications have long been recognized in lung cancer. Genomic profiling studies of NSCLC, using FISH, have revealed focal copy number alterations of the chromosomal area of known oncogenes, such as FGFR1 (8p12), SOX2 (3q26.3–q27), PIK3CA (3q26.3), MET (7q31.2), and EGFR (7p12.2)[11–15]. In our study, the profile of these genetic alterations according to different histological types of lung cancer was consistent with that of previous studies (Supplementary Table S2 online). The expression of SGOL1-B was increased specifically in lung cancer with focal copy number amplifications. Our *in vitro* studies also suggest that the overexpression of SGOL1-B in lung cancer may cause genomic instability (Supplementary Table S3 online). Thus, we hypothesized that SGOL1-B-positive cancer could be predisposed to genomic instability. The reasons for the amplifications of focal genomic areas are not known and have been

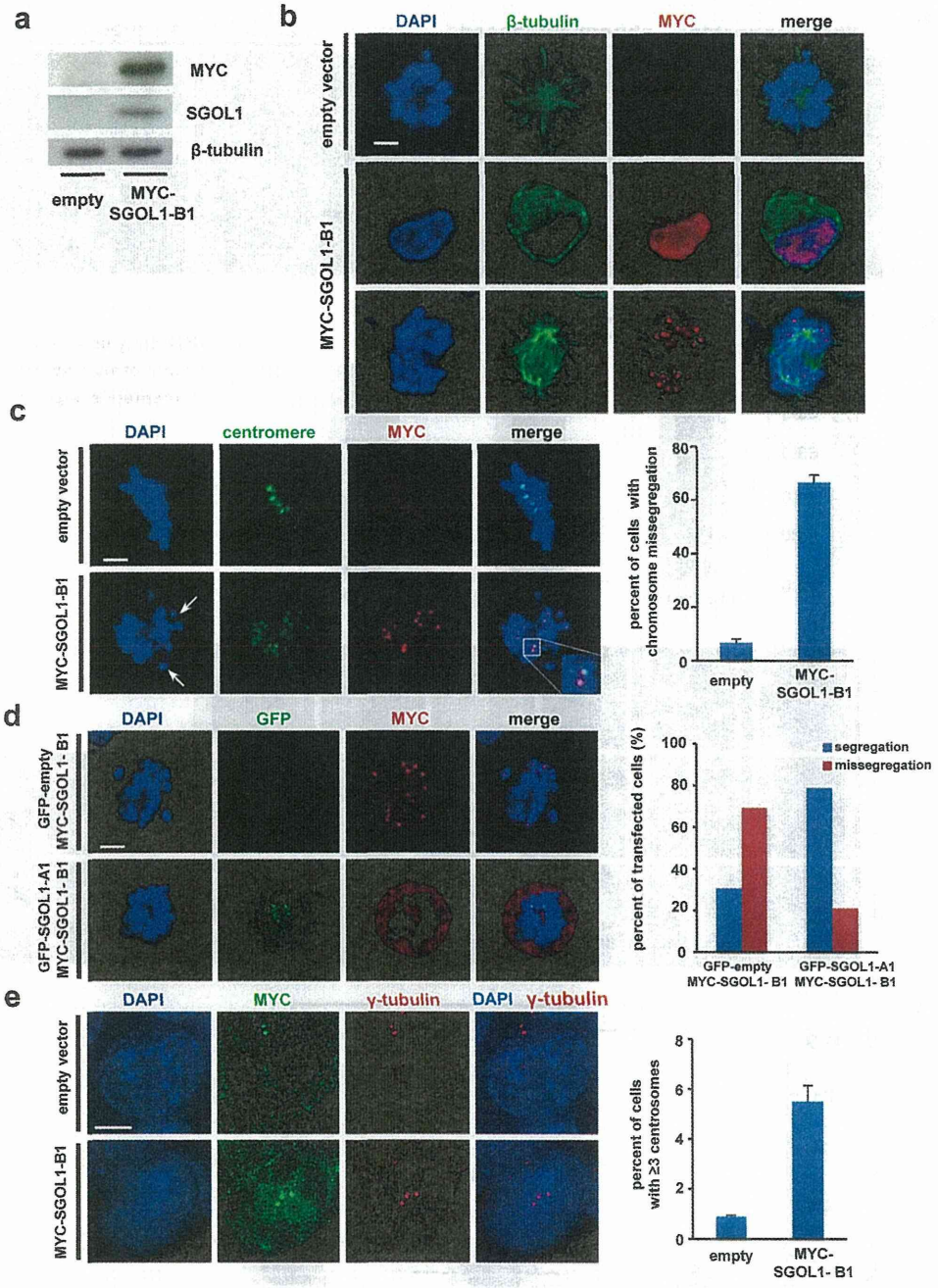


**Figure 2 | Centromeric localization and aberrant chromosome alignment during mitosis in lung cancer cells expressing SGOL1-B1.** (a) Ectopic expression of SGOL1-B1 in the human NSCLC cell line ACC-LC-176. The cells were transfected with the expression vector for MYC-SGOL1-B1, and the cellular extracts were subjected to a western blot analysis. Cropped images are shown and original whole gels and cropped lines are in Supplementary Figure S2 online. (b) Localization of SGOL1-B1 during the cell cycle. Cells at interphase (middle panels) and prophase-metaphase (lower panels) are shown using staining for MYC-SGOL1-B1 (*red*), β-tubulin (*green*) and DNA (*blue*). (c) Centromeric localization of SGOL1-B1. ACC-LC-176 cells were transfected with an empty vector or a MYC-SGOL1-B1 expression vector, and after synchronization to metaphase using nocodazole, the cells were stained with an anti-MYC antibody (*red*), anti-centromere antibody (*green*) and DAPI (*blue*). The inset shows a magnified image of the centromere. The mitotic cell expressing MYC-SGOL1-B1 (*lower panels*) shows chromosome missegregation. An attached graph shows percentage of cells exhibiting chromosome missegregation. The results are presented as ($n = 50$) from three independent experiments. (d) Rescue of SGOL1-B1-derived missegregation phenotype by the overexpression of SGOL1-A1 in NSCLC cells. ACC-LC-176 cells were transfected with GFP-empty or GFP-SGOL1-A1 vector together with the MYC-SGOL1-B1 expression vector. At 20 h post-transfection, the cells were synchronized to metaphase with nocodazole, fixed, and stained with an anti-MYC antibody (*red*) and DAPI (*blue*). Chromosome missegregation is shown in the upper panels, while the chromosomes were properly segregated in the lower panels. Scale bar = 5 μm. Statistical analysis of misaligned chromosomes in experiment. Results are presented ($n = 50$) from three independent experiments. (e) Centrosome amplification detected in ACC-LC-176 cells expressing SGOL1-B1. The cells were transfected with an empty vector or a MYC-SGOL1-B1 expression vector, and at 48 h post-transfection, the cells were stained with an anti-MYC antibody (*green*), anti-γ-tubulin (*red*), and DAPI (*blue*). Scale bar = 5 μm. An attached graph shows percentage of cells exhibiting centrosome amplification. Results are presented ($n = 200$) from three independent experiments.

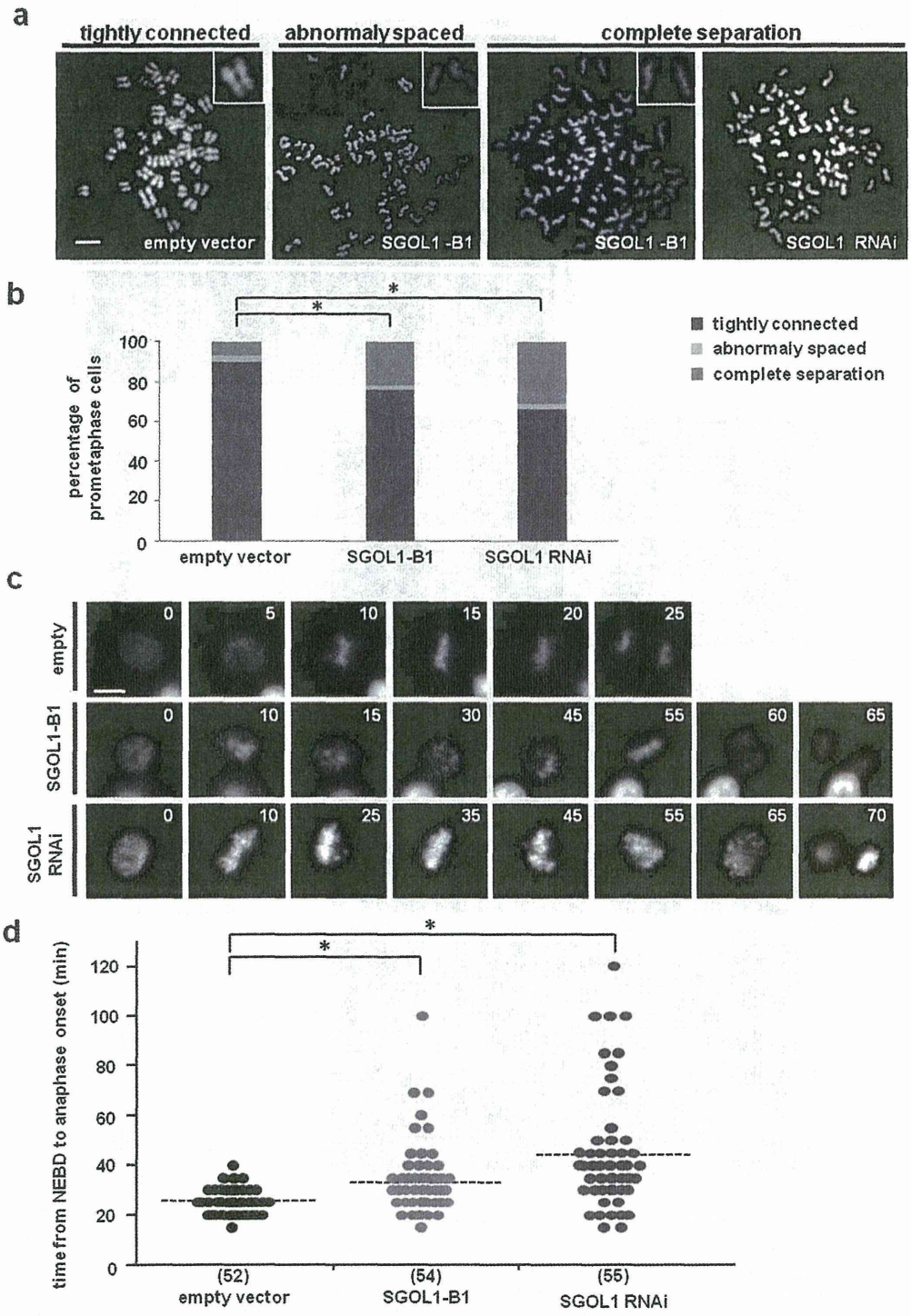


**Figure 3 | Cohesion defects between sister chromatids and delayed mitotic progression in lung cancer cells expressing SGOL1-B1.** (a) Representative images of chromosome spread exhibiting cohesion defects. The NSCLC cell line ACC-LC-176 was transfected with GFP-H2B expression vector together with the MYC-SGOL1-B1 expression vector, SGOL1 shRNA vector, or control vector. The cells were then treated with nocodazole to arrest the cell cycle during mitosis, and the chromosomes were spread, stained with DAPI, and classified into the following three patterns: (I) tightly connected pattern, normal cohesive chromatids or only a very few pairs of separated sister chromatids; (II) abnormally spaced pattern, separated chromatids have remained in close proximity to the pair partner (several chromatid pairs remain cohesive); and (III) complete separation pattern, severely separated chromatids (the pair partner is often hard to identify because it is located some distance away). (b) Percentage of cells with cohesion defects between sister chromatids in experiment (a). $*P < 0.05$ (Fisher exact test). (c) Detection of delayed mitotic progression in ACC-LC-176 cells transfected with vectors as described in (a) using time-lapse analysis. The mitotic progression time was defined as the elapsed time from NEBD to anaphase onset. Images were acquired every 5 min. The elapsed time in minutes is shown at the upper right of each panel. Scale bar = 10 μm. (d) Quantitation of the mitotic progression time in experiment (c). Each symbol in the scatter plot represents a single cell. The solid horizontal bars represent the median values. $*P < 0.0005$ [Mann-Whitney *U*-test]. The numbers of examined cells are indicated in parentheses.

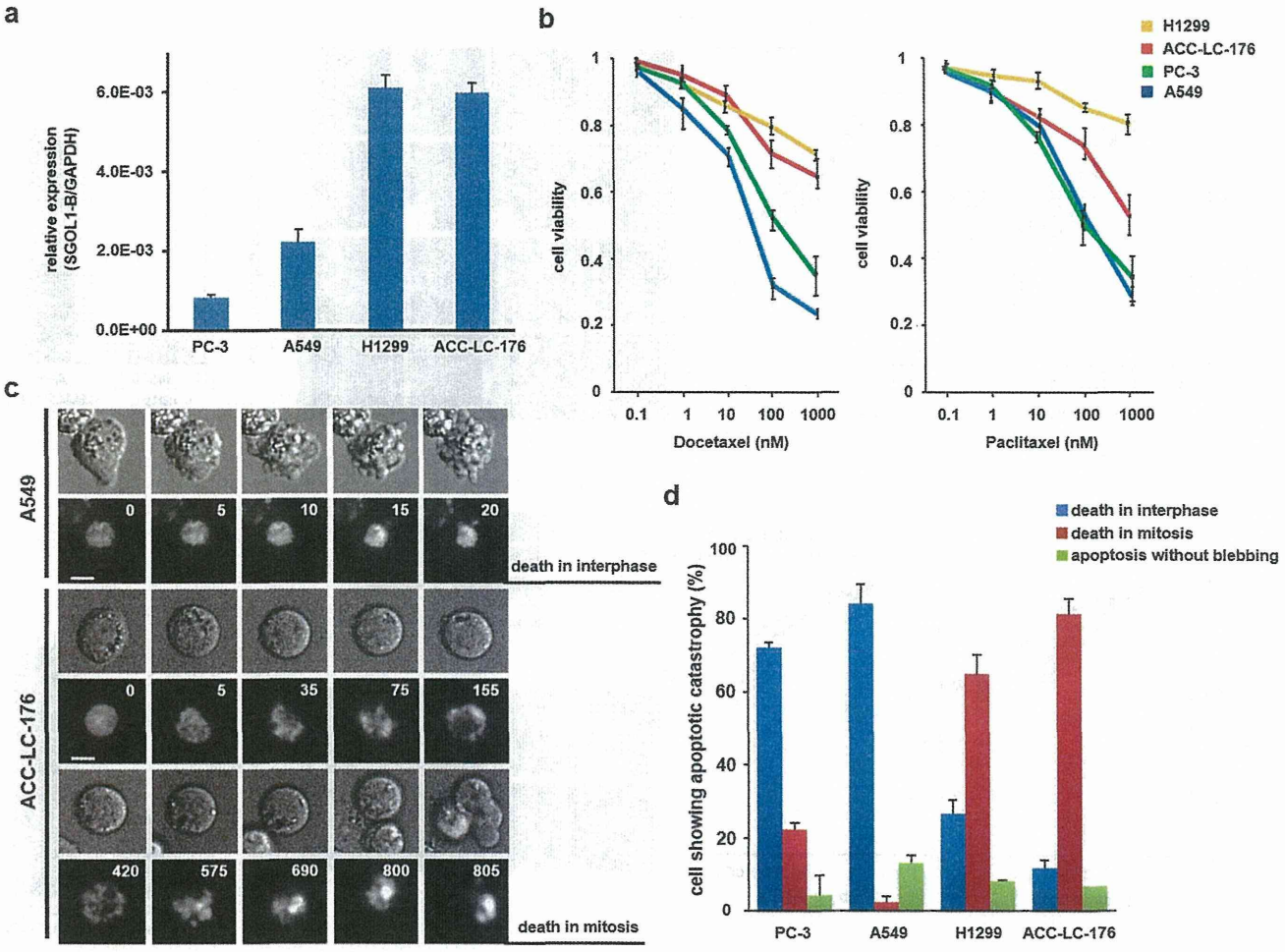


**Figure 4 | Difference in taxane responses of WT EGFR NSCLC cell lines according to their SGOL1-B expression level.** (a) SGOL1-B mRNA expression levels determined using quantitative real-time RT-PCR in three NSCLC cell lines with WT EGFR and a cell line with EGFR mutation. The data shown are the mean of at least three independent experiments. (b) Responses of PC-3, A549, H1299 and ACC-LC-176 cells to docetaxel and paclitaxel treatment as evaluated using a WST-8 colorimetric assay. (c) Representative images of time-lapse sequences illustrating the two types of death after exposure to docetaxel. Scale bar = 10 μm. The number at the upper right of each panel indicates the time in minutes. (d) Percentages of PC-3, A549, H1299 and ACC-LC-176 cells exhibiting various cell fates in response to 1,000 nM of docetaxel.

sparsely addressed in previous literature. Our observation may imply that a guardian of mitosis control and its aberrant spliced product may bring about global instability in the genome, causing the amplification of particularly sensitive regions of the chromosomes[22,23].

Our present study revealed a new and important role of SGOL1-B in lung cancer progression. The overexpression of SGOL1-B has been associated with centrosome amplification. Multiple spindle poles have been reported to be common in mitotic SGOL1-knockdown cells and the cell expressing SGOL1-P1[2,4,24]. In a lung cancer cell line transfected with SGOL1-B, considerable amount of centrosome amplification was noted. Several studies have demonstrated a relationship between exposure to carcinogens implicated in lung cancer and the development of centrosome abnormalities *in vitro*[25,26]. SGOL1 is required for the protection of centromeric cohesion from prophase to the metaphase-anaphase transition until all the kinetochores have been properly captured by the spindle microtubules[27]. In SGOL1-B1 overexpressed cells, the weakness of centromere protection induces accurate chromosome missegregation on the metaphase plate, leading to mitotic delay. This result is consistent with the observation that cells expressing SGOL1-B showed a high frequency of mitotic cells with premature centromere separation that were delayed at the G2/M transition[3]. Cells with SGOL1-B overexpression, which showed a cancer tissue-specific expression in primary lung cancer, induced aberrant mitosis, which accelerated the acquisition of further malignant phenotypes. On the other hand, in terms of concurrent centrosome amplification associated with SGOL1-B overexpression as described above, centrosome proteins like PLK4 and Tpx2 are also known to be involved with generation of aberrant mitosis, the same phenotype shown here. Actually, a high frequency of mitotic errors are notable in lung cancer cells spontaneously occurring in mice heterozygous for PLK4 and Tpx2[28,29]. Our study showing that the overexpression of SGOL1-B is observed in lung cancer provides a new and important link between aberrant mitosis and lung carcinogenesis.

Taxanes are among the most widely used antitumor agents in the treatment of NSCLC. Our data clearly showed that SGOL1-B upregulation was associated with a more intractable subset of NSCLC. A lung cancer cell line that overexpressed SGOL1-B exhibited an aberrant dynamicity in response to taxanes. Taxanes successfully kill tumor cells during mitosis by targeting microtubules and disrupting normal chromosome movement[30]. This effect occurs because the primary effect of taxanes is to bind to microtubules, thereby decreasing mitotic dynamicity. Thus, this cell line expressing SGOL1-B is thought to be more prone to overcoming the effects of taxanes on

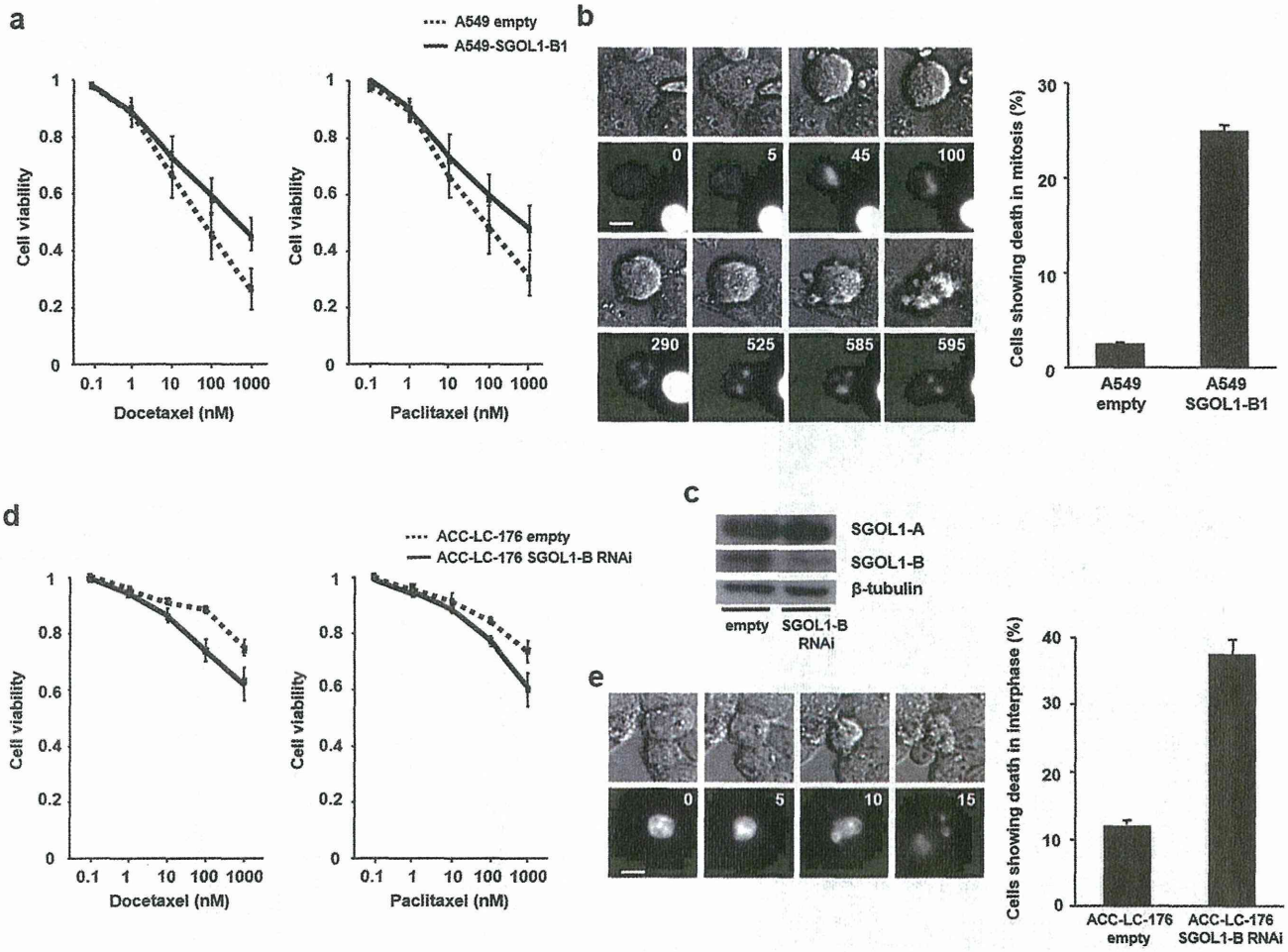


**Figure 5 | Expression level of SGOL1-B defines the response to docetaxel.** (a) Responses of empty vector (mock)- and SGOL1-B1-transfected A549 NSCLC cells to docetaxel and paclitaxel as evaluated using a WST-8 colorimetric assay. The data shown are the mean of at least three independent experiments. (b) Representative images of "death in mitosis" in A549 cells overexpressing SGOL1-B1 detected using time-lapse microscopy. Scale bar = 10 μm. An attached graph shows percentages of mock- and SGOL1-B1 expression vector-transfected A549 cells exhibiting "death in mitosis" in response to 1,000 nM of docetaxel. (c) Western blot analysis of expression of SGOL1-B in ACC-LC-176 NSCLC cells after shRNA knockdown for SGOL1-B was inside the graph.Cropped images are shown and the original whole gels are available in Supplementary Figure S3 online. (d) Responses of mock vector- and SGOL1-B shRNA expression vector-transfected ACC-LC-176 cells to docetaxel and paclitaxel as evaluated using a WST-8 colorimetric assay. The data shown are the mean of at least three independent experiments. (e) Representative images of "death in interphase" of SGOL1-B-knockdown ACC-LC-176 cells detected using time-lapse microscopy. Scale bar = 10 μm. An attached graph shows percentages of mock- and SGOL1-B shRNA expression vector-transfected ACC-LC-176 cells exhibiting "death in interphase" in response to 1,000 nM of docetaxel.

microtubule dynamics. It is tempting to speculate that the assessment of SGOL1-B expression might be a predictive marker for taxane-based chemotherapy. Until now, several markers are proposed as predictors of responses to taxane therapy[31,32]. Especially, high levels of βIII-tubulin expression in NSCLC are associated with low response rates and poorer survival in patients treated with chemotherapies based on anti-mitotic agents[33–35]. Our data indicate that a taxane-resistant lung cancer cell line expresses higher mRNA levels of a specific SGOL1 splice variant, SGOL1-B. The determination of the SGOL1-B mRNA level may be useful for selecting subjects who are likely to benefit from chemotherapy based on taxanes.

The molecular pathways resulting in taxane-induced cell death without mitosis entry ("death in interphase") or death in response to aberrant mitosis ("death in mitosis") remain unclear[17,36]. In our study, lung cancer cells with a high expression level of SGOL1-B were more resistant to mitotic arrest induced by taxane than other cell lines with a low expression level of SGOL1-B. Although mitotic arrest is a hallmark cellular response to taxane, previous studies have shown that the antitumor efficacy of paclitaxel is dependent on its ability to induce apoptosis, not mitotic arrest[37]. Another study with NSCLC A549 cells also found that low concentrations of paclitaxel are sufficient to induce cell death without an apparent G2-M block[38]. These reports strongly support our result that A549, which had a low expression level of SGOL1-B, was taxane-sensitive. The expression level of SGOL1-B may alter cellular fate profiles.

We do not know exactly what produced the multitude of genetic changes in lung cancer cases with SGOL1-B overexpression. Our analysis may provide an insight that abnormal mitosis in response to an elevated SGOL1-B level posits the cancer cells as having a high frequency of focal copy number amplifications. NSCLC cells with a high expression level of SGOL1-B that were exposed to taxane underwent mitotic arrest. The mechanism of taxane-resistance might be associated with abnormal mitosis induced by SGOL1-B and mitotic arrest induced by taxane. These findings underlie the importance of determining the SGOL1-B expression status, which could be used in addition to the EGFR status in the selection of candidates for